Journal of Anatomy

J. Anat. (2019) **235**, pp189–204 doi: 10.1111/joa.13007

A digital dissection of two teleost fishes: comparative functional anatomy of the cranial musculoskeletal system in pike (*Esox lucius*) and eel (*Anguilla anguilla*)

Robert Brocklehurst,[1,2] Laura Porro,[2,3] Anthony Herrel,[4] Dominique Adriaens[5] and Emily Rayfield[2]

[1]*School of Earth and Environmental Sciences, University of Manchester, Manchester, UK*
[2]*School of Earth Sciences, University of Bristol, Bristol, UK*
[3]*Department of Cell and Developmental Biology, University College London, London, UK*
[4]*UMR 7179 (MNHN-CNRS) MECADEV, Département Adaptations du Vivant, Muséum National d'Histoire Naturelle, Paris, France*
[5]*Department of Biology, Evolutionary Morphology of Vertebrates, Ghent University, Gent, Belgium*

Abstract

Advances in X-ray computed tomography (CT) have led to a rise in the use of non-destructive imaging methods in comparative anatomy. Among these is contrast-enhanced CT scanning, which employs chemical stains to visualize soft tissues. Specimens may then be 'digitally dissected', producing detailed, three-dimensional digital reconstructions of the soft- and hard-tissue anatomy, allowing examination of anatomical structures *in situ* and making accurate measurements (lengths, volumes, etc.). Here, we apply this technique to two species of teleost fish, providing one of the first comprehensive three-dimensional (3D) descriptions of teleost cranial soft tissue and quantifying differences in muscle anatomy that may be related to differences in feeding ecology. Two species with different feeding ecologies were stained, scanned and imaged to create digital 3D musculoskeletal reconstructions: *Esox lucius* (Northern Pike), predominantly a suction feeder; and *Anguilla anguilla* (European eel), which captures prey predominantly by biting. Muscle cross-sectional areas were calculated and compared between taxa, focusing on muscles that serve important roles in feeding. The adductor mandibulae complex – used in biting – was larger in *Esox* than *Anguilla* relative to head size. However, the overall architecture of the adductor mandibulae was also very different between the two species, with that of *Anguilla* better optimized for delivering forceful bites. Levator arcus palatini and sternohyoideus – which are used in suction feeding – are larger in *Esox*, whereas the levator operculi is larger in *Anguilla*. Therefore, differences in the size of functionally important muscles do not necessarily correlate neatly with presumed differences in feeding mode.
Key words: contrast-enhanced CT; cranial osteology; feeding; myology; Teleostei.

Introduction

Teleost fishes make up approximately half of vertebrate diversity (Nelson, 2006), with over 31 000 living species and new species being described every year (Eschmeyer & Fong, 2013); they occupy a huge variety of ecological niches and exhibit a wide range of morphological and behavioural adaptations (Helfman et al. 2009). A major source of variation in teleosts is the diverse array of feeding modes employed by different species. The majority of teleosts (like most aquatic animals) capture their prey using suction feeding (Wainwright et al. 2015), in which expansion of the buccal cavity through elevation of the neurocranium, depression of the hyoid and lateral expansion of the suspensorium creates a negative pressure inside the mouth. The resulting pressure gradient draws prey into the mouth and through the oral cavity for swallowing (Lauder, 1985; Westneat, 2006; Day et al. 2015).

Suction feeding is believed to be the ancestral feeding mode of teleosts, and some groups (e.g. Cypriniformes, Acanthomorpha) have become highly specialized for suction feeding (Wainwright et al. 2015). Another major feeding mode within teleosts is biting, capturing prey items by grasping them firmly in the oral jaws (Alfaro et al. 2001;

Correspondence
Robert Brocklehurst, School of Earth and Environmental Sciences, University of Manchester, Michael Smith Building, Oxford Road, Manchester, M13 9PT, UK.
E: robert.brocklehurst-2@postgrad.manchester.ac.uk

Accepted for publication *29 March 2019*
Article published online *30 May 2019*

Mehta & Wainwright, 2007a). Biting behaviours frequently involve removing pieces of prey items, circumventing the constraints that maximum gape size places on prey size in suction feeders (Alfaro et al. 2001).

Biting and suction feeding are often presented as a dichotomy, but this is misleading as the use of biting does not preclude suction generation (Alfaro et al. 2001). Some biting taxa use suction to position prey, and almost all biters retain suction capacity for intra-oral transport (with a few derived exceptions, e.g. moray eels; Mehta & Wainwright, 2007b). Biting and suction feeding place differing functional demands on the skull and jaws, which are predicted to strongly influence the form of the cranial musculoskeletal system (Barel, 1982; Liem, 1990; Wainwright et al. 2004; but see Van Wassenbergh et al. 2007a,b).

Biting is powered by the action of the adductor mandibulae complex (Alfaro et al. 2001), which is responsible for jaw closure. Suction feeding is powered by the axial musculature, with the epaxial and hypaxial muscles driving expansion of the buccal cavity through multiple musculoskeletal linkages (Camp & Brainerd, 2014; Camp et al. 2015). Whilst previous models of suction feeding posited major roles for the cranial and hyoid muscles – the levator arcus palatini, levator opercula and sternohyoideus – in the linkages responsible for lateral and ventral cranial expansion (Liem, 1980a; Lauder, 1982, 1985; Westneat, 2006), new measurements have shown that most (if not all) of the power comes from the axial musculature (Camp et al. 2015). Nevertheless, the cranial and hyoid muscles are likely to still have an important role over the precise control of suction-feeding kinematics, which will affect prey capture efficiency (Camp & Brainerd, 2015).

There have been several broad surveys of teleost musculoskeletal anatomy (Gregory, 1933; Greenwood, 1971; Winterbottom, 1973; Datovo & Vari, 2013, 2014), as well as detailed descriptive (Geerinckx & Adriaens, 2007; Huysentruyt et al. 2007; Leysen et al. 2011) and functional studies (Herrel et al. 2002; Van Wassenbergh et al. 2005; Goulet et al. 2016) focusing on specific taxa. However, these data are almost exclusively presented in two dimensions as either photographs or line drawings, and so are limited in the amount of information they can subsequently convey on 3D muscle orientation and topology. This, in turn, limits the accuracy of functional inferences that can be drawn (e.g. bite force estimates; Lautenschlager, 2013).

Contrast-enhanced computed tomography (CT) scanning is a technique that has become increasingly popular in comparative anatomy, allowing non-destructive imaging of both hard and soft tissues, and has been shown to produce excellent resolution in both small and large vertebrate specimens (Jeffery et al. 2011; Gignac et al. 2016; Fig. 1). Specimens are stained with contrast-enhancing agents prior to scanning that are taken up differentially by soft tissues, improving soft-tissue resolution and allowing

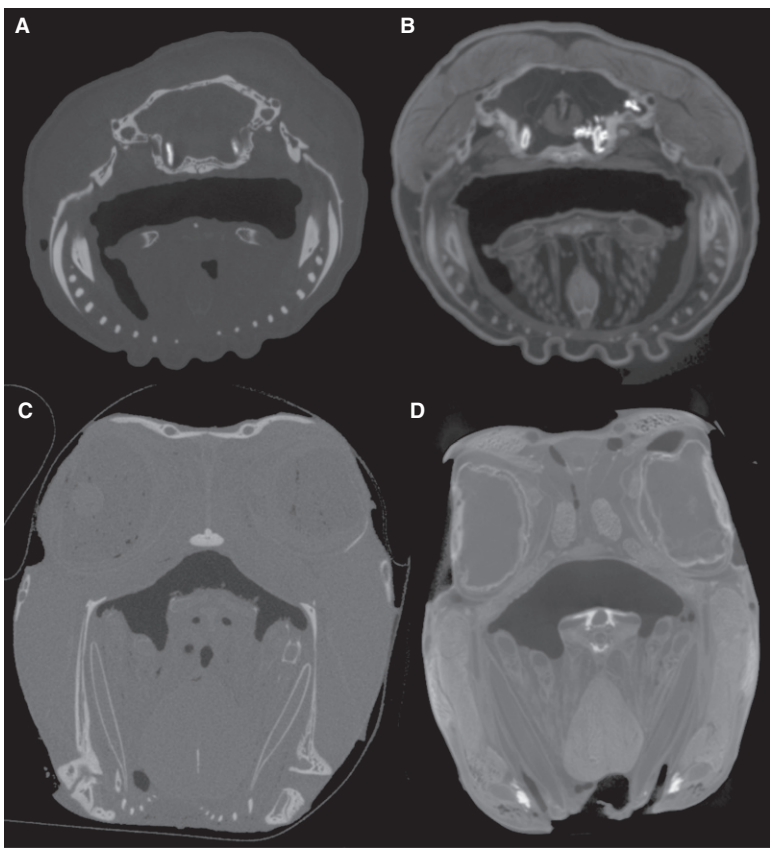

Fig. 1 Comparison of coronal computed tomography (CT) slices showing transverse sections of *Anguilla anguilla* (A, B) and *Esox lucius* (C, D), and specimens before (A, C) and after (B, D) contrast-enhancement staining. Images not to scale.

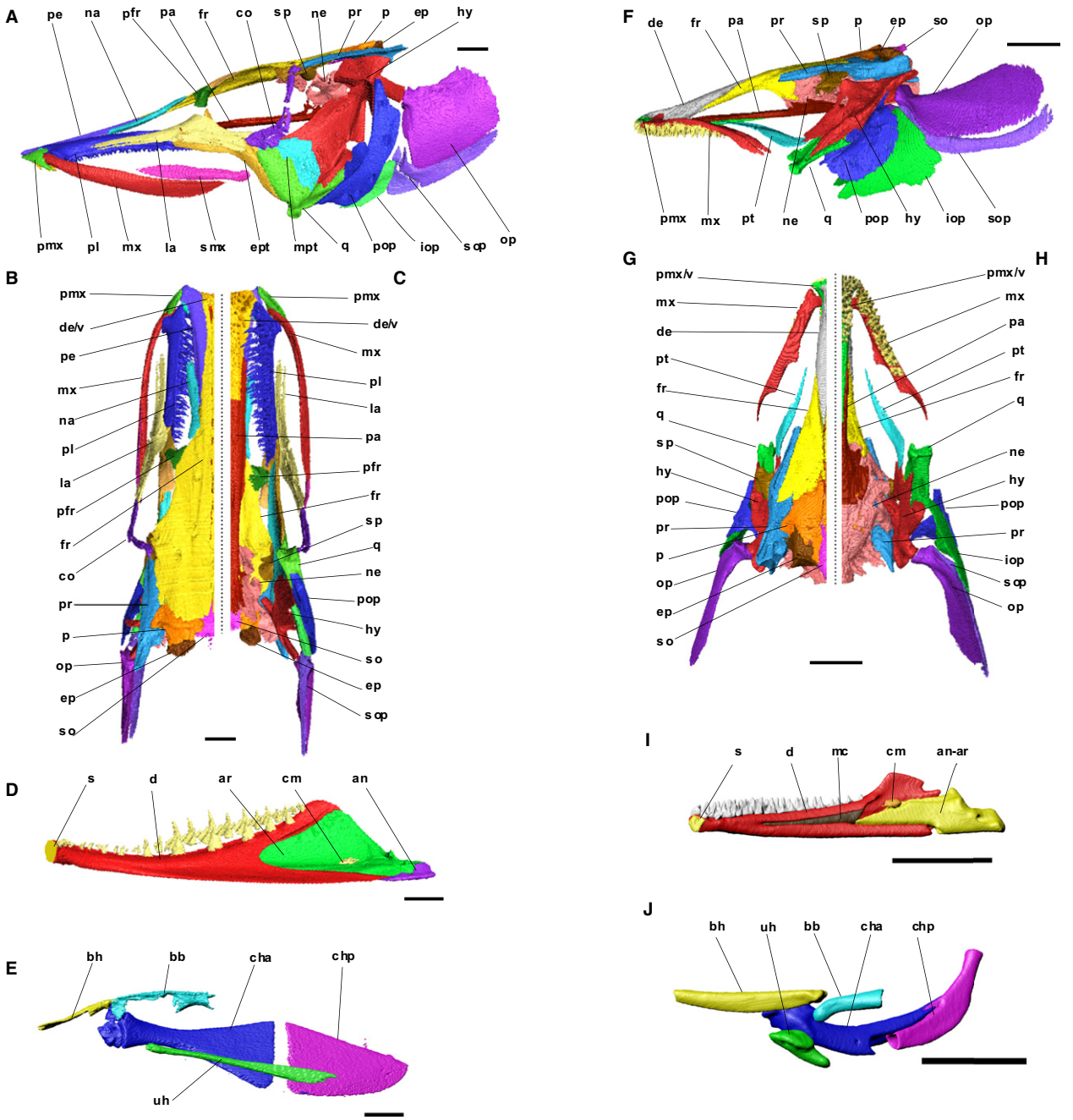

Fig. 2 Cranial, mandibular and hyoid osteology of *Esox* (A–E) and *Anguilla* (F–J). Skulls in lateral (A, F), dorsal (B, G) and ventral (C, H) views with lower jaw removed. Lower jaws (D, I) and hyoids (E, J) in medial view. Scale bars: 5 mm. an, angular; an-ar, angulo-articular; ar, articular; bb, basibranchial; bh, basihyal; cha, anterior ceratohyal; chp, posterior ceratohyal; cm, coronomeckelian; co, circumorbital series; d, dentary; de, dermethmoid; de/v, fused dermethmoid and vomer; ep, epitotic; ept, ectopterygoid; fr, frontal; hy, hyomandibular; iop, inter-opercular; la, lacrimal; mc, Meckel's cartilage; mpt, metapterygoid; mx, maxilla; na, nasal; ne, neurocranium; op, opercular; p, parietal; pa, parasphenoid; pe, proethmoid; pfr, pre-frontal; pl, palatal; pmx, pre-maxilla; pmx/v, fused pre-maxilla and vomer; pop, pre-opercular; pr, pterotic; pt, pterygoid; q, quadrate; s, symphysis; smx, supra-maxilla; so, super-occipital; sop, sub-opercular; sp, sphenotic; uh, urohyal.

differentiation of tissue types (Descamps et al. 2014; Gignac et al. 2016). As a result, contrast-enhanced CT scans have been used to 'digitally dissect' specimens, producing interactive three-dimensional (3D) virtual anatomical atlases (Holliday et al. 2013; Lautenschlager et al. 2014; Porro & Richards, 2017), and provide useful functional data on soft tissue, for example, muscle volumes (Cox & Faulkes, 2014; Sharp & Trusler, 2015).

To date, this method has mostly been applied to tetrapods (Cox & Jeffery, 2011; Holliday et al. 2013; Lautenschlager et al. 2014; Sharp & Trusler, 2015; Porro & Richards, 2017), but there are examples of contrast-enhanced CT and 'digital dissection' of teleosts (De Meyer et al. 2018a). Although several studies have presented 3D reconstructions of teleost anatomy both graphically (Anker, 1974; Adriaens & Verraes, 1996a,b) and digitally (Leysen et al. 2011; Bouilliart et al. 2015), these are almost all based on destructively sampled histological data; the non-destructive nature of contrast-enhanced CT makes it an attractive option, and the digital anatomical models can be readily used in biomechanical modelling applications (Cox et al. 2011; Orsbon et al. 2018).

In order to better understand the link between skull form and function in teleosts, specimens of two taxa with different feeding modes were subjected to contrast-enhanced CT scanning – the Northern Pike (*Esox lucius* Linnaeus 1758), predominantly a suction feeder, and the European eel (*Anguilla anguilla* Linnaeus 1758), which predominantly uses biting. Both taxa are piscivorous and adapted to taking fairly large prey. In addition, neither possesses extreme morphological specializations for their preferred feeding mode, for example, the protrusible upper jaws of suction-feeding Cypriniformes and Acanthomorpha (Wainwright et al. 2015), or the raptorial pharyngeal jaws of biting Morinoguids (Mehta & Wainwright, 2007b), making them more directly comparable.

The musculoskeletal anatomy of the skull and hyoid is reconstructed in 3D to produce digital dissections of these two teleosts (Figs 2–7). In order to perform quantitative comparisons between species with different feeding mechanisms, muscle volume and cross-sectional area (CSA) were measured for functionally important muscle groups and compared between *Esox* and *Anguilla*. Given the differences in predominant feeding mode between these two taxa, it is hypothesized that the jaw adductor muscles that power biting would be larger in *Anguilla,* and the suspensorial, opercular and hyoid muscles that control suction feeding would be larger in *Esox*. In addition to testing these specific hypotheses, the detailed digital dissections provide additional data on musculoskeletal architecture that may be of functional relevance.

Materials and methods

A sub-adult *Esox* [head length (HL) measured from the anterior edge of the premaxilla to the posterior edge of the epiotic = 60 mm] and an adult *Anguilla* (HL = 26 mm) were used in this study. *Anguilla anguilla* exhibits a broad vs. narrow head shape dimorphism, which is related to diet (Ide et al. 2011; De Meyer et al. 2018a,c); the specimen used in this study was a broad-headed individual, which are more piscivorous. The *Esox* specimen was micro (μ)CT scanned at the Imaging and Analysis Centre at the Natural History Museum (London, UK) on a X-Tek HMX-ST μCT 255 scanner (Nikon Metrology, Tring, UK) at 180 kV and 120 μA with a 0.5-mm copper filter producing 1999 TIFF images with a resolution of 0.043 mm voxel^{-1}. Afterwards, the *Esox* specimen was fixed in 4% buffered paraformaldehyde solution and stained using a 10% I_2KI solution for 7 days. Following staining, the *Esox* head was briefly rinsed with 90% ethanol (to wash excess stain from the skin) and scanned at 185 kV and 180 μA with a 0.1-mm copper filter producing 1999 TIFF images with a resolution of 0.043 mm voxel^{-1}. The *Anguilla* specimen was preserved in 4% buffered formalin solution and scanned at the UGCT Department at the University of Ghent (Belgium) with the HECTOR μCT scanner at 120 kV and 117 μA, producing 1170 TIFF images at a resolution of 0.07 mm voxel^{-1}. The head was then stained in a 5% solution of phosphomolybdic acid (PMA) for 29 days, then scanned again at 120 kV and 260 μA, producing 668 TIFF images at a resolution of 0.07 mm voxel^{-1}.

All CT data were imported into Avizo 7.0–8.0 (FEI Visualization Sciences Group, OR, USA). Bones were separated from soft tissues in the unstained datasets using automatic thresholding, although some manual segmentation was necessary to separate individual bones from each other. Segmentation of soft-tissue structures in the stained dataset was performed manually. For each taxon, the two datasets (unstained and stained) were aligned and merged to create single musculoskeletal models containing all hard and soft tissues using landmarks visible in both datasets.

For the quantitative comparison across the two taxa, muscle volumes were computed using the 'Material Statistics' module in Avizo. Muscle volumes were divided by muscle length to obtain estimates for CSA for the adductor mandibulae muscles. Total muscle length was used here as an approximation for muscle fibre length, measured using the standard Measure tools in Avizo, as pennation angle (and hence physiological CSA) could not be readily determined from the stained CT scan data. To account for differences in specimen size, the results for *Anguilla* were scaled to those of a specimen with the same cranial volume (defined as the volume enclosed by the head for all slices anterior to the occipital condyle) as the *Esox* specimen. Finally, a correction factor was applied to the *Esox* muscle measurements as I_2KI is known to cause soft-tissue shrinkage (Vickerton et al. 2013). This correction factor was derived through comparison of total tissue volume and CSA in the unstained and stained *Esox* datasets. Hard-tissue volume was computed from the unstained dataset, and total cranial volume for both the stained and unstained datasets using the 'Material Statistics' module in Avizo. Soft-tissue volumes pre- and post-staining were then calculated by subtracting hard-tissue volume from these totals. Soft-tissue volume decreased by 35% as a result of staining, and CSA decreased by 25%. No correction was necessary for the *Anguilla* data, as PMA does not cause noticeable soft-tissue shrinkage (Descamps et al. 2014). CSA (proportional to muscle force output) was compared for the adductor mandibulae complex, and muscle volumes (proportional to muscle power output) were compared for the adductor mandibulae, as well as the suspensorial, opercular and hyoid muscles. Three muscles of particular interest are the levator arcus palatini, the levator operculi and the sternohyoideus, all of which are hypothesized to play roles in suction feeding.

Results

Osteology

The osteology of the skull in teleosts has been described extensively (Gregory, 1933). For a brief illustrated summary of the various skull bones of *Esox* and *Anguilla*, which are

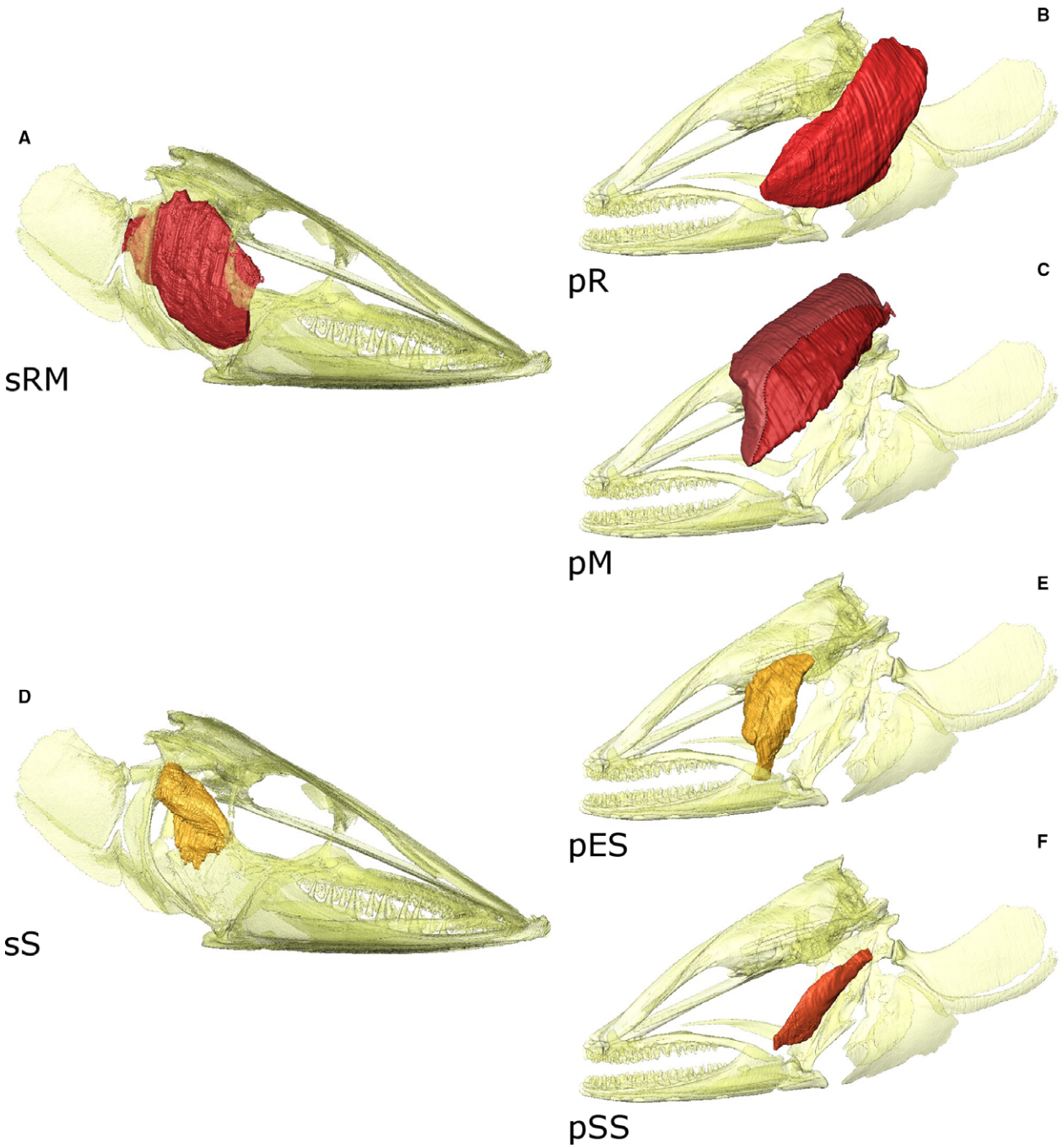

Fig. 3 Individual muscles of the adductor mandibulae segmentum facialis in *Esox* (A, D) and *Anguilla* (B, C, E, F), in oblique views. *Esox* rictomalaris section, sRM (A) and stegalis section, sS (D). *Anguilla* pars rictalis, pR (B); pars malaris, pM, with division into pro- and retro-malaris indicated by the dotted line (C); pars epistegalis, pES (E); pars substegalis, pSS (F). Images not to scale.

referenced during the descriptions of the cranial muscles, see Fig. 2.

Cranial musculature

Adductor mandibulae

Following the nomenclature of Datovo & Vari (2013), the adductor mandibulae is divided into two segments: a facial segment, the segmentum facialis (Fig. 3); and a mandibular segment, the segmentum mandibularis (Fig. 4).

Segmentum facialis. In teleosts, the segmentum facialis consists of three parts: the pars malaris, pars rictalis and pars stegalis (Fig. 3). The pars rictalis forms the ventro-lateral portion, the pars malaris forms the dorso-lateral portion, and the pars stegalis forms the medial portion. In

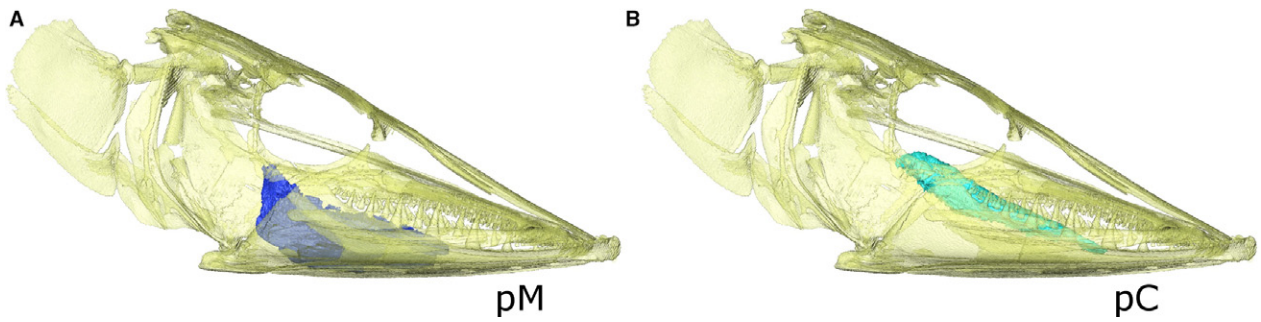

Fig. 4 Individual muscles of the adductor mandibulae segmentum mandibularis (AMSM) in *Esox* shown in oblique view. Pars coronalis, pC (A); pars mentalis, pM (B).

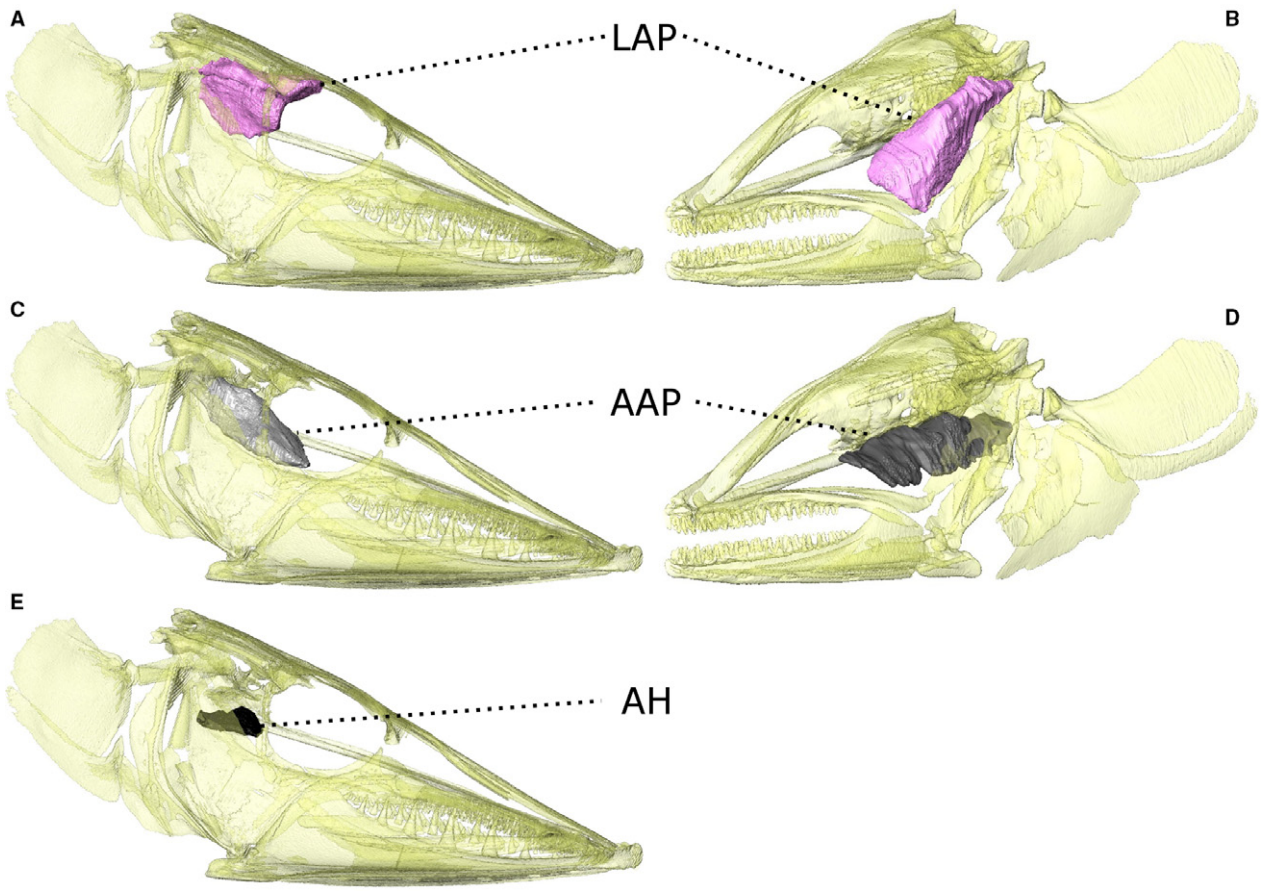

Fig. 5 Individual suspensorial muscles of *Esox* (A, C, E) and *Anguilla* (B, D), in oblique view. Levator arcus palatini, LAP (A, B); adductor arcus palatini, AAP (C, D); adductor hyomandibulae, AH (E). Images not to scale.

some taxa, including *Esox*, the rictalis and malaris form a compound facial segment, the ricto-malaris (Datovo & Vari, 2014). In *Anguilla*, the rictalis and malaris segments share a common origin, but are divided anteriorly into distinct parts (Datovo & Vari, 2014), and so are discussed separately here. Additionally, the pars stegalis may be differentiated into a dorso-lateral epistegalis portion and a medio-ventral substegalis portion. This division is present in *Anguilla*, but in *Esox* there is only a single undivided stegalis section (Datovo & Vari, 2014).

Pars rictalis and malaris—The ricto-malaris in *Esox* originates ventral to the levator operculi, adductor operculi and dilator operculi muscles, lateral to the stegalis. The origin site covers multiple bones of the suspensorium, including ventral and lateral portions of the hyomandibula, the medial side of the anterodorsal portion of the preopercula, and the lateral side of the quadrate. A group of fibres originating from the posterior process of the hyomandibula pass through the ovoid fenestra bounded by the hyomandibula and preopercula. The

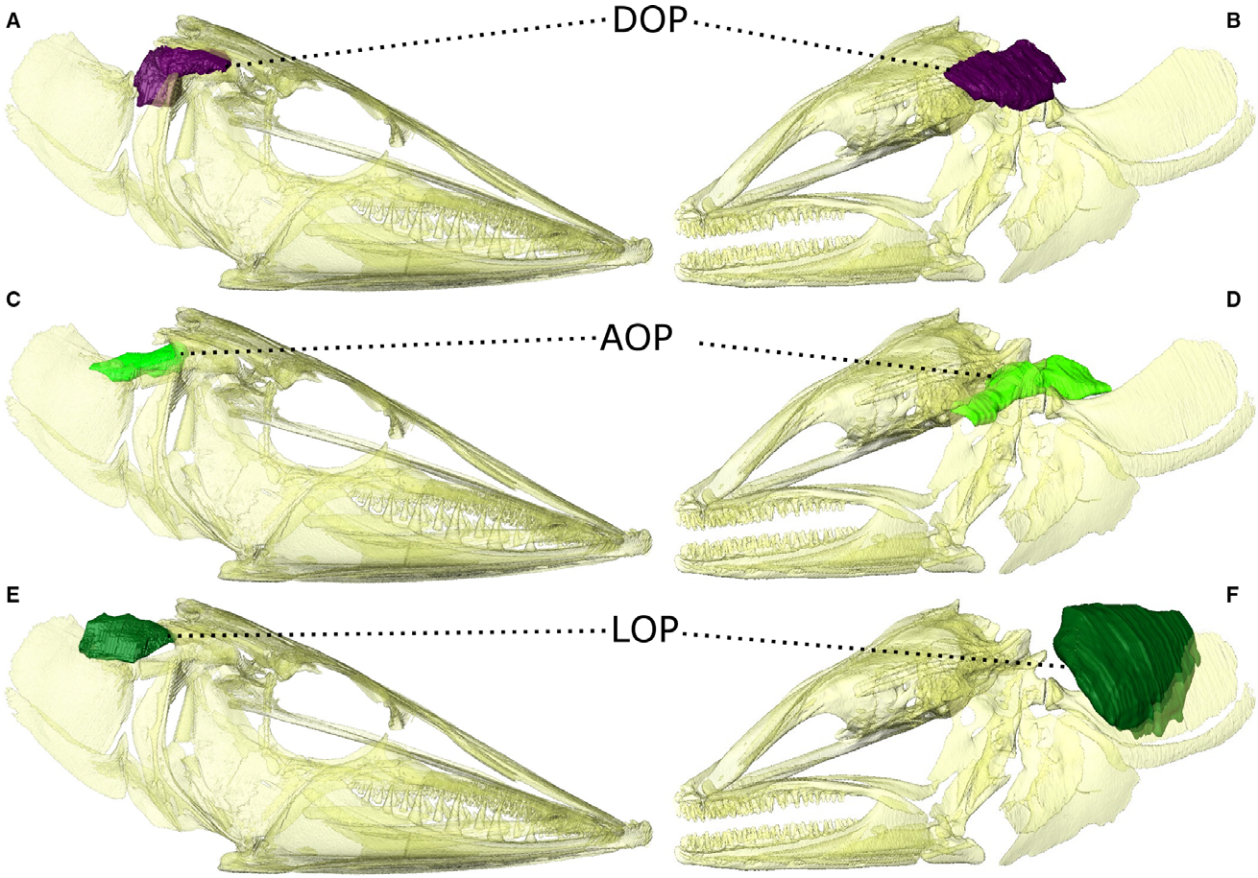

Fig. 6 Individual opercular muscles of *Esox* (A, C, E) and *Anguilla* (B, D, F), in oblique view. Dilator operculi, DOP (A, B); adductor operculi, AOP (C, D); levator operculi, LOP (E, F). Images not to scale.

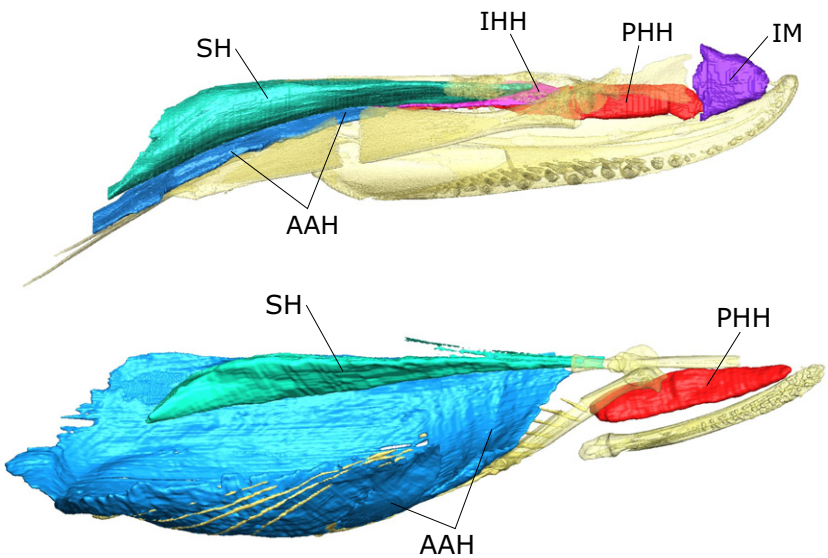

Fig. 7 Three-dimensional (3D) visualizations of the hyoid musculature of *Esox* (top) and *Anguilla* (bottom). AHH, abductor and adductor hyohyoidei; IHH, inferior hyohyoidei; IM, intermandibularis; PHH, protractor hyoidei; SH, sternohyoideus. Images not to scale.

remaining fibres, which form the main body of the muscle, are directed anteriorly, lateral to the stegalis and palatal muscles. In *Esox,* the ricto-malaris inserts onto the medial side of the dentary and angulo-articular via the mandibular tendon and the mandibular raphe, at the level of the coronoid process.

In *Anguilla*, the origin of the rictalis covers the dorsal portions of the preopercula, the lateral side of the posterior portion of the hyomandibular body, and the lateral surface of the pterotic. The muscle fibres are directed anteroventrally, ventral to the malaris and lateral to the dilator operculi (posteriorly) and the stegalis (anteriorly). The fibres of the rictalis insert onto the lower jaw via the intersegmental aponeurosis and a large tendinous sheet, attaching to the coronoid process of the dentary. The malaris muscle in *Anguilla* is subdivided into a retromalaris and promalaris (Datovo & Vari, 2014). Both subdivisions share the epaxialis and supra-cranial fasciae as part of their origin sites but, additionally, the promalaris originates from the frontals, parietals and the mid-sagittal tendinous raphe, whereas the retromalaris originates from the pterotic (Datovo & Vari, 2014). The whole malaris section inserts onto the lower jaw via the mandibular tendon.

Pars stegalis—The stegalis segment of *Esox* originates from the metapterygoid, and the anterior portions of the hyomandibula, medial to the rictomalaris, travelling along the lateral side of the anteriorly projecting hyomandibular arm. The fibres of the stegalis are directed anteriorly, and the stegalis inserts onto the lower jaw via the Meckelian tendon, which attaches to the coronomeckelian bone.

In *Anguilla*, the epistegalis has its origin on the lateral surface of the pterotic and anterior face of the sphenotic. The substegalis originates from the lateral side of the hyomandibula (within the 'fork' of the two processes that contact the quadrate). The fibres of both the epistegalis and substegalis travel anteroventrally, but whilst the epistegalis inserts directly onto the medial surface of the dentary and articular, the substegalis inserts onto the coronomeckelian bones via the Meckelian tendon.

Segmentum mandibularis. The segmentum mandibularis is made up of two parts: the pars coronalis and the pars mentalis (Fig. 4). In *Esox*, this entire section originates from the mandibular raphe (Datovo & Vari, 2014), a band of connective tissue that separates the mandibular and facial segments of the adductor mandibulae. In *Anguilla*, the segmentum mandibularis is completely absent.

Pars coronalis—The pars coronalis forms the dorsal part of the segmentum mandibularis in *Esox*. It attaches to the dorsal surface of Meckel's cartilage, as well as the dorsomedial aspect of the dentary.

Pars mentalis—The pars mentalis forms the ventral part of the segmentum mandibularis in *Esox*. It attaches to the ventro-medial aspect of the dentary and Meckel's cartilage.

Suspensorial musculature

The three major muscles are the levator arcus palatini, the adductor arcus palatini and the adductor hyomandibulae (Fig. 5).

Levator arcus palatini. The levator arcus palatini serves to laterally expand the buccal cavity through abduction of the suspensorium. In both *Esox* and *Anguilla,* this muscle originates from the ventral surface of the sphenotic, posterior to the eyeball. In *Esox*, the muscle fibres are directed posteriorly, inserting on the dorsomedial side of the anterior arm of the hyomandibula, and on the anterior portions of the hyomandibular body.

In *Anguilla*, the fibres of the levator arcus palatini 'fan out' from their origin on the ventral sphenotic, and insert posteriorly onto the lateral side of the hyomandibular body, mid-way onto the anterior arm of the hyomandibular, and anteriorly onto pterygoids.

Adductor arcus palatini. The adductor arcus palatini is responsible for suspensorial adduction. The muscle originates on the postero-ventral portion of the parasphenoid and ventro-lateral sides of the braincase in *Esox*, ventral to the eyeball. The muscle is directed posteriorly, and terminates ventral to adductor operculi, inserting onto the medial side of the hyomandibular body and the dorsal portion of metapterygoid.

The origin site is similar in *Anguilla*; the ventral margins of the braincase and lateral edges of the postero-ventral body of the parasphenoid. The muscle inserts on the medial side of the hyomandibula (attaching to the anteriorly projecting 'arm').

Adductor hyomandibulae. In *Esox*, the adductor hyomandibulae origin lies posterior to that of the adductor arcus palatini, on the posterior ventral surface of the parasphenoid and ventrolateral parts of the braincase. The adductor hyomandibulae travels posterolaterally towards its insertion on the medial side of the hyomandibula and metapterygoid, at the contact between the two bones. This muscle is absent in *Anguilla* (De Schepper et al. 2007).

Opercular muscles

The three major muscles are the dilator operculi, the adductor operculi and the levator operculi (Fig. 6).

Dilator operculi. The dilator operculi is responsible for opercular abduction. In *Esox*, this muscle originates from the ventrolateral surface of the pterotic (dorsal to the levator arcus palatini). The fibres of the dilator operculi then

run for a short distance posteriorly to insert on the articular head of the opercular bone.

In *Anguilla*, the dilator operculi origin site covers the posterolateral portions of the pterotic and sphenotic, dorsal to the origination sites of the pars substegalis and levator arcus palatini. The dilator operculi muscle then passes posteriorly, medial to the rictalis, ventral to the malaris, dorsolateral to the adductor operculi. The dilator operculi then insert onto the dorsolateral part of the anterior process of the opercular that contacts the hyomandibula.

Adductor operculi. The adductor operculi is responsible for opercular adduction. In *Esox*, this muscle has its origins on the posterior parts of the neurocranium and the posterior half of the medial side of the hyomandibular body and posterior arm. The muscle fibres course posteriorly, dorsomedial to the rictalis, medial to the dilator operculi, and ventromedial (then ventral) to the levator operculi. It then inserts onto the antero-medial faces of the main body of the opercular bone.

The adductor operculi originates from the ventral surface of the pterotic in *Anguilla*, dorsal to the adductor arcus palatini and ventromedial to the origins of the levator arcus palatini. The muscle fibres run posteriorly and flare laterally, medial to the levator operculi. The muscle inserts onto the medial side of the hyomandibular body and the medial part of the anterior process of the opercular.

Levator operculi. The levator operculi of *Esox* originates from the posterior edge of the hyomandibular body and the posteroventral edges of the pterotic, dorsolateral to the adductor operculi, and dorsomedial to the dilator operculi. The muscle is directed posteriorly, dorsolateral to adductor operculi and inserts along the dorsolateral edge of the opercular bone – the insertion site of the levator operculi continues further posteriorly than that of the adductor operculi.

The levator operculi in *Anguilla* originates from the ventrolateral margins of the pterotic and the postero-lateral faces of the hyomandibular body, ventral to the rictalis. The muscle then passes posteriorly, flares dorso-ventrally lateral to the opercular, and inserts onto the lateral face of the main opercular body.

Hyoid muscles

The major hyoid muscles include the intermandibularis, protractor hyoidei, inferior hyohyoideus, adductor hyohyoideus and sternohyoideus (Fig. 7).

Intermandibularis. This muscle in *Esox* connects the left and right dentaries, stretching transversely between the two halves of the lower jaw. It is absent in Anguilla.

Protractor hyoidei. In *Esox*, this muscle originates posterior to the intermandibularis from the medial surface of the dentary. The fibres then travel posteriorly to insert onto the lateral and ventrolateral faces of the anterior ceratohyal. In *Anguilla*, the protractor hyoidei also originates from the medial surface of the dentary, just posterior to the mandibular symphysis and inserts onto the lateral face of the posterior ceratohyal.

Inferior hyohyoideus. In *Esox*, this muscle originates from the midline and ventrolateral aspect of the urohyal. The fibres run dorsolaterally and insert onto the ventrolateral face of the anterior ceratohyal. It is absent in *Anguilla*.

Abductor and adductor hyohyoidei. The abductor and adductor hyohyoidei surround the gill chamber. The abductor runs from the midline to the first branchiostegal ray,

Table 1 Muscle CSA and volume data for the adductor mandibulae complex of *Anguilla* and *Esox*.

	Muscle CSA (mm^2)		Muscle volume (mm^3)	
	Anguilla	*Esox*	*Anguilla*	*Esox*
Segmentum facialis				
Rictomalaris section				
Pars rictalis	40.0 (37%)	67.1 (50%)	942 (39%)	1500 (50%)
Pars promalaris	30.8 (28%)		791 (32%)	
Pars retromalaris	17.3 (16%)		415 (17%)	
Stegalis section				
Pars epistegalis	13.6 (12%)	23.4 (17%)	194 (8%)	307 (10%)
Pars substegalis	7.3 (7%)		108 (4%)	
Segmentum mandibularis				
Pars coronalis	N/A	13.1 (10%)	N/A	397 (13%)
Pars mentalis	N/A	31.1 (23%)	N/A	808 (27%)

Data for *Anguilla* have been scaled to account for head size differences with the *Esox* specimen. *Esox* data have been corrected for shrinkage caused by the iodine staining. N/A indicates that that particular muscle is either absent or could not be distinguished from another muscle. Values reported to three significant figures. CSA, cross-sectional area.

and the adductor then runs between all subsequent branchiostegal rays. These muscles are much larger in *Anguilla* than in *Esox* due to the greatly expanded branchiostegal rays.

Sternohyoideus. The sternohyoideus is a large muscle, which connects the pectoral girdle to the hyoid apparatus in both *Esox* and *Anguilla*. It is composed of left and right halves, which originate from the left and right cleithra, respectively, and inserts anteriorly onto the urohyal via a well-developed tendon. In *Anguilla*, this muscle is partially covered by the expanded adductor hyohyoidei.

Muscle functional comparison

After correcting for head size differences and soft-tissue shrinkage caused by the staining process, both the total CSA and volume of the adductor mandibulae complex are greater in *Esox*. However, if only the segmentum facialis is considered, then muscle volume and CSA are larger in *Anguilla* (Table 1; Fig. 8). In both taxa, the stegalis section is the smallest part of the adductor mandibulae, making up <20% of jaw adductor muscle CSA (Table 1; Fig. 8). In *Anguilla*, all of the remainder (81%) is made up of the pars rictalis and subdivided pars malaris. In *Esox*, the presence of the segmentum mandibularis makes a significant contribution (Fig. 8), accounting for 33% of the CSA of the adductor mandibulae, with the ricto-malaris section making up the remainder (50%; Table 1). Similar patterns are seen when muscle size is measured in terms of volume (Table 1). In terms of muscle division, although *Esox* possesses the additional segmentum mandibularis, the segmentum facialis has far more divisions in *Anguilla* than *Esox*.

All of the suspensorial muscles are larger in *Esox* than in *Anguilla* but, in particular, the levator arcus palatini, which is involved in suction feeding (Table 2; Fig. 9). Also, when comparing the relative sizes of the suspensorial abductors – the levator arcus palatini – and adductors – the adductor arcus palatini and adductor hyomandibulae – the abductors are significantly larger in *Esox*, but in *Anguilla* the two muscle groups are of roughly equal size (Table 2).

The opercular muscles, by contrast, are larger in *Anguilla* than in *Esox* overall (Table 2). This is due entirely to the greatly enlarged levator operculi, which is responsible for dorsal rotation of the operculars (Table 2; Fig. 9). Both the adductor operculi and dilator operculi – which adduct and abduct the operculars, respectively – are larger in *Esox* than in *Anguilla* (Table 2; Fig. 9).

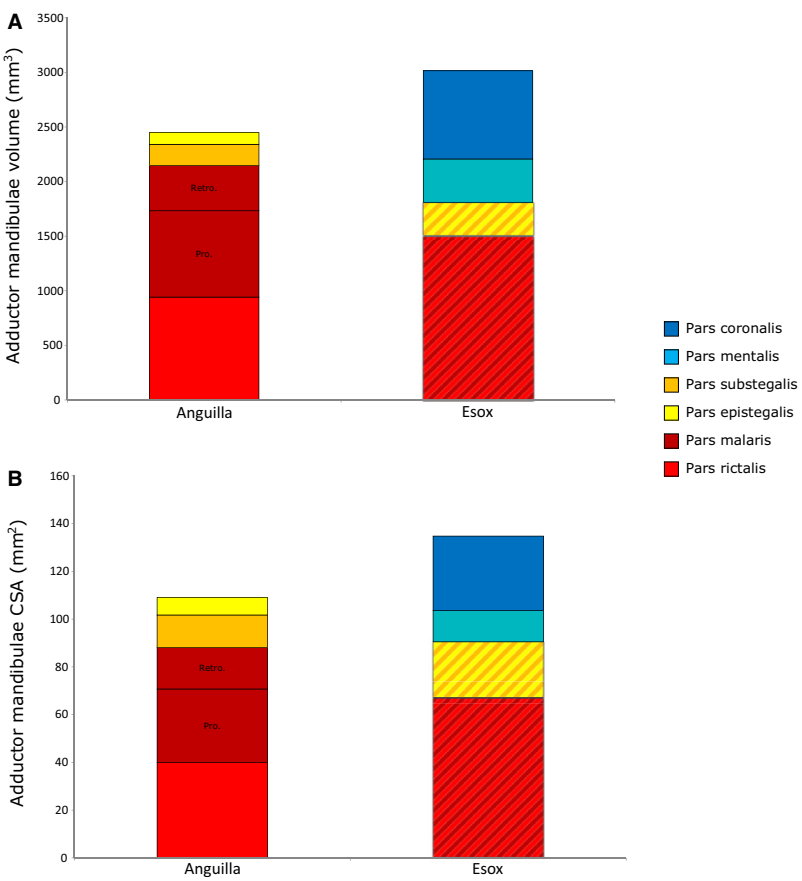

Fig. 8 Graphs showing the cross-sectional area (CSA) and volume for the adductor mandibulae complex of *Anguilla* and *Esox,* following corrections for differences in head size and possible soft-tissue shrinkage. Hatching indicates compound sections. Individual muscles are colour coded as in the three-dimensional (3D) reconstructions.

Table 2 Muscle volume data (in mm^3) for the suspensorial, opercular and hyoid muscles of *Anguilla* and *Esox*.

	Esox	*Anguilla*
Suspensorial muscles		
Adductor arcus palatini	451	229
Adductor hyomandibulae	72.3	N/A
Levator arcus palatini	618	244
Opercular muscles		
Dilator operculi	167	145
Adductor operculi	158	109
Levator operculi	155	360
Hyoid muscles		
Intermadibularis	53.4	N/A
Protractor hyoidei	321	280
Hyohyoid inferior	57.4	N/A
Adductor hyohyoideus	384	2540
Sternohyoideus	1450	1190

Data for *Anguilla* have been scaled to account for head size differences with the *Esox* specimen. *Esox* data have been corrected for shrinkage caused by the iodine staining. N/A indicates that that particular muscle is either absent or could not be distinguished from another muscle. Values reported to three significant figures.

Anguilla has a greater volume of hyoid musculature overall than *Esox*, although this is due to the greatly expanded adductor hyohyoidei associated with the enlarged branchiostegal rays (Table 2; Figs 7 and 9). The most important muscle for suction feeding is the sternohyoideus; this muscle is larger in *Esox* than in *Anguilla* (Table 2). The protractor hyoidei, which is involved in generating suction for respiration (Osse, 1968), is also larger in *Esox* (Table 2). The hyoid musculature of *Esox* is also more complex, with several additional muscles – the intermandibularis and the hyohyoideus inferior – that are not present in *Anguilla* (Figs 7 and 9).

Discussion

The results presented here demonstrate some interesting – and in some cases unexpected – patterns in the anatomy of the cranial musculature with respect to feeding mode. As the two taxa here are not radically specialized for solely biting or suction feeding, it would be premature to try and generalize these results to all biting and suction-feeding fishes; more studies are needed on a greater range of taxa, and the division between 'biters' and 'suction-feeders' is somewhat arbitrary, although relative specializations certainly do exist (Ferry et al. 2015). Still, this demonstrates how the two taxa involved in our study have both solved the problem of piscivory in very different ways – one mainly relying on biting, the other mainly on suction – and how this has influenced the evolution of the cranial musculoskeletal system.

Differences in size and arrangement of the adductor mandibulae

Our hypothesis that the biting taxon *Anguilla* would have larger jaw-closing muscles than the suction-feeding taxon *Esox* does not seem to be supported by the data presented here. Both the volume and CSA of the adductor mandibulae are greater in *Esox,* which utilizes suction feeding to a greater extent than *Anguilla*. It has been reported that the adductor mandibulae is typically larger in taxa that capture prey primarily by biting rather than suction (Turingan & Wainwright, 1993; Alfaro et al. 2001), and so the observed pattern may seem surprising. However, differences in specific feeding styles (and their functional demands) used by each taxon could be explained by more subtle differences in anatomy than overall adductor muscle size. Eels use biting as well as suction (Mehta & Wainwright, 2007a,b) for capturing small prey, but rely on the production of high bite forces in order to remove pieces from large prey items and break into armoured small prey (Proman & Reynolds, 2000; De Meyer et al. 2018b,c). Pike use suction to capture small prey (Rand & Lauder, 1981); large prey are initially drawn into the mouth by suction, then bitten into and grasped with the teeth, before being moved through the oral cavity and swallowed using subsequent suction events, resulting in a ratcheting effect (LB Porro, A Herrel, personal observations).

Bite force and jaw-closing velocity are dependent on muscle CSA as well as the orientation of a muscle's line of action (Herrel et al. 2002; Van Wassenbergh et al. 2005). The larger adductor mandibulae in *Esox* is due to the presence of an additional segment, the segmentum mandibularis, which has an almost horizontal orientation and makes up ~ 40% of the adductor mandibulae CSA. This segment is absent in *Anguilla*. In contrast, both the volume and CSA of the other portion of adductor mandibulae, the more vertically oriented segmentum facialis, are greater in *Anguilla* than in *Esox*. The segmentum facialis also has finer subdivisions in *Anguilla* than *Esox*, perhaps suggesting the entire muscle needs to be more functionally flexible, or that finer control is needed during biting or processing. An additional consideration is that these results do not account for muscle pennation, as this could not be reliably determined from the CT data. The muscles in *Anguilla* are pennate with short fibres, whereas *Esox* has long fibres and low pennation angles. As a result, we would expect *Anguilla* to be capable of producing higher bite forces than *Esox,* particularly at low gape angles. This is in agreement with bite force data collected *in vivo* (Dutel et al. 2015; De Meyer et al. 2018b). By contrast, the longer fibres of *Esox* should permit a larger range of movement and wider gape angles.

As *Esox* utilizes suction feeding to a greater extent, we might expect the feeding system to be more adapted to rapid opening and closing of the jaws to quickly capture prey (Barel, 1982). The substantial mass of the segmentum

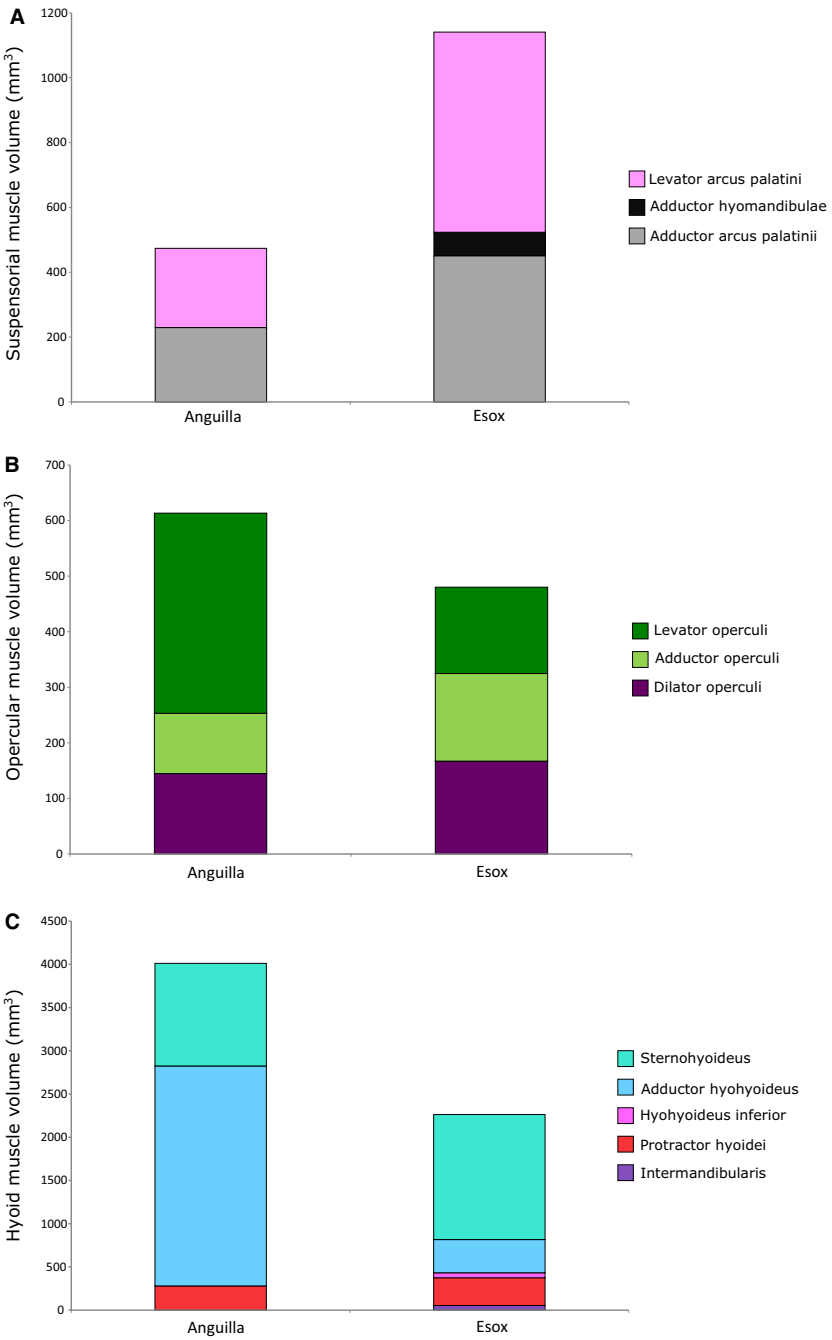

Fig. 9 Graphs showing the volume for the suspensorial, opercular and hyoid muscles of *Anguilla* and *Esox,* following corrections for differences in head size and possible soft-tissue shrinkage. Individual muscles are colour coded as in the three-dimensional (3D) reconstructions.

mandibularis of *Esox* likely functions to facilitate fast jaw closing at high gape angles during suction feeding on large prey, when the muscle fibres are vertically oriented. The increased posteriorly-directed force generated by the segmentum mandibularis at lower gape in *Esox* may also be advantageous, resisting anteriorly-directed forces produced when grasping struggling prey. Additionally, *Esox* has proportionally longer jaws than does *Anguilla*, which decreases the mechanical advantage of the jaw adductor muscles but also increases jaw-closing velocity (more characteristic of suction feeders; Wainwright et al. 2004; Westneat, 2004).

A final difference in the organization of the jaw musculature between these two taxa is the connection between the adductor mandibulae and the epaxial musculature found in *Anguilla*. In addition to 'standard' biting behaviour, *Anguilla* is known to engage in rotational feeding, or 'death-roll' style behaviour, whereby the jaws clamp firmly onto a prey item and the eel then spins its body via contraction of the axial musculature in order to tear pieces off when scavenging (Helfman & Clark, 1986; De Schepper et al. 2005). During such behaviour, the linkage between the axial muscles and the jaw adductors may be highly advantageous,

increasing force transmission to the lower jaws and, hence, bite forces, although this hypothesis still requires further testing.

Differences in size and arrangement of the 'suction' muscles

Suction feeding is a complex process, involving multiple musculoskeletal linkages, including the cranial muscles, but also the axial musculature (Lauder, 1985; Westneat, 2006; Camp et al. 2015; Day et al. 2015). Therefore, it is difficult to make inferences about suction-feeding performance based on cranial musculature alone. Classic models of suction-feeding mechanics proposed important roles in suction generation for three cranial muscles: the levator arcus palatini, levator operculi and sternohyoideus (Liem, 1980a; Lauder, 1982, 1985; Westneat, 2006). Even though it is now known that these muscles do not contribute strongly to generating the power for suction feeding (Camp et al. 2015), they still play an important role in kinematic control.

The levator arcus palatini, which controls lateral flaring of the suspensorium and expansion of the buccal cavity (Lauder, 1985; Westneat, 2006), is larger in *Esox* than in *Anguilla*. This may permit greater control over suction strike kinematics, which will impact feeding performance (Day et al. 2015). Control over the lateral aspect of buccal cavity expansion though contraction of the levator arcus palatini could be particularly useful during asymmetric strikes (Liem, 1980b) when attempting to catch more elusive prey. Alternatively, it may help *Esox* to manipulate and position larger prey items that cannot be fully ingested in one suction event.

The levator operculi controls mouth opening through the opercular four-bar mechanism – dorsal rotation of the opercular retracts the interopercular bone and the ligament connecting this bone to the lower jaw (Lauder, 1980; Van Wassenbergh, 2005). Despite being thought to be important for suction feeding, this muscle is larger in *Anguilla*. This may be due to the fact that these muscles are also active during ventilation, and the large jaw adductor muscles of the segmentum facialis in *Anguilla* stiffen the suspensorium, increasing the load the levator operculi needs to work against. Whilst it is possible the levator operculi is enlarged in *Anguilla* due to this role in gill ventilation, the other opercular muscles do not follow the same pattern; the dilator operculi is similarly sized in both taxa, and the adductor operculi is smaller in *Anguilla* than in *Esox*.

An additional complication in *Anguilla* is that the epaxial muscles are mechanically coupled to the adductor mandibulae (presumably an adaptation to torsional feeding; Liem, 1980a; De Schepper et al. 2005), contacting the pars malaris via a tendinous sheet. This means that the power generated through contraction of the epaxial muscles, rather than solely driving neurocranial elevation as in other teleosts, is being transmitted to the mandible to elevate the lower jaws and assist during biting. Therefore, whilst this mechanism may increase bite force in *Anguilla*, the epaxial muscles may also be contributing less than they otherwise would towards neurocranial elevation and lower jaw depression; however, the precise mechanics of this linkage require further investigation. One possible explanation for the large levator operculi in *Anguilla* may be that there is an increased reliance on this muscle to power jaw opening; an alternative is that it may serve to stabilize the operculars against the action of the epaxial musculature, as well as preventing damage from rotational movements during rotational feeding.

Comparing the hyoid muscles, the protractor hyoidei is of equivalent size in the two taxa, and the abductor and adductor hyohyoidei are greatly expanded in *Anguilla*, as they sheath the lengthened branchiostegal rays. The ventral cranial musculature of *Esox* includes two additional (but small) muscles not present in *Anguilla*; the intermandibularis and the hyohyoideus inferior. The functional roles for these muscles remain unclear. The presence of the intermandibularis in *Esox* may assist in resisting the forces produced by struggling prey and resisting stress at the mandibular symphysis. The inferior hyohyoidei is involved in the adduction of the ceratohyals, and so it may be linked to either control of hyoid kinematics during suction feeding, or during prey processing.

The sternohyoideus has the biggest role in suction feeding of the hyoid muscles, as it controls ventral expansion of the buccal cavity through hyoid depression and drives lower jaw rotation via the mandibulohyoid ligament (Lauder, 1980; Aerts, 1991). However, it has been shown that this muscle in fact lengthens during the expansive phase of suction feeding, and is mainly acting as ligament to transmit power generated by the hypaxial musculature (Van Wassenbergh et al. 2007a,b; Camp & Brainerd, 2015). Therefore, power generated by the active shortening of the sternohyoideus must be involved in other behaviours such as prey processing and transport. The sternohyoideus has been shown to exhibit asymmetric activity during prey processing in bony fishes (Lauder & Norton, 1980), and this may be particularly important for *Esox* to manipulate and position large prey that require multiple suction events to fully ingest.

The cranial and hyoid musculature involved in suction feeding plays an important role in force and power transmission from the axial muscles, and the control of suction-feeding kinematics (Camp et al. 2015). However, because these muscles are not actually generating power, it is possible that muscle volume is not the most relevant functional metric. CSA may be more relevant as this relates to the muscle's force transmission ability, especially if the muscle in question is transmitting force via eccentric or isometric contraction, as is the case for the sternohyoideus (Van Wassenbergh et al. 2007a,b; Camp & Brainerd, 2015). If CSA for the cranial muscles involved in suction feeding can predict the

amount of force they are transmitting, then this could potentially be used to estimate cranial expansion and suction power. However, this hypothesis would require further testing, as well as more detailed investigations into the axial muscles themselves and how the power they generate is transmitted through the cranial and hyoid linkages.

Conclusions

Contrast-enhanced CT scanning and 'digital dissection' are promising methods in comparative anatomy and are here applied to teleosts, the most diverse group of living vertebrates. In addition to permitting the highly detailed description of the soft-tissue anatomy in these taxa *in situ*, such digital approaches lend themselves to quantification, allowing easy, non-destructive (and hence repeatable) measurements of the musculoskeletal system, which can then be used in further computational biomechanical analyses. Iodine has received the greatest attention as a tool for contrast-enhanced CT; however, if precise soft-tissue quantification is desired, then alternative staining agents, such as PMA, should be considered, as iodine staining protocols are still being optimized to reduce potential tissue shrinkage.

Esox, which feeds primarily using suction, has a larger adductor mandibulae complex, despite *Anguilla* primarily using biting as its main feeding mode. However, biting performance is not determined by the size of the jaw adductors alone and, in *Anguilla,* the more vertical orientation and greater structural complexity of the muscles likely improve biting performance compared with *Esox*. The increased size of the levator arcus palatini in *Esox* may serve a role during breathing. Alternatively, along with the enlarged sternohyoideus, it could be related to suction feeding, but its role (if any) is more likely to be fine kinematic control rather than power production, which is provided by the axial musculature. The larger levator operculi in *Anguilla* may also serve a respiratory role, but other possible functions include stabilization of the operculum during rotational feeding, or assisting in mouth opening. Whilst these are interesting possibilities, further functional studies are required in order to fully understand the implications of these observed anatomical differences.

Acknowledgements

The authors thank J. Christiaens and B. De Kegel for preparing the eel specimens. The authors are greatly indebted to D. Sykes (Imaging and Analysis Centre, Natural History Museum, London) and M. Dierick & L. Van Hoorebeke (UGCT Department at the University of Ghent, Ghent, Belgium) for performing the μCT scanning. S. Lautenschlager and T. Davies provided technical assistance with AVIZO. Preparation and scanning of the pike specimen was part of a Marie Curie International Incoming Research Fellowship ('Tetrapods Rising', 303161) to LBP. Preparation and scanning of the eel specimens was part of a project funded by UGent Special Research Fund (project 01J05213) to DA.

Author contributions

LBP and EJR conceived of and designed the project. AH provided specimens of *Esox*. LBP stained and CT scanned the specimen of *Esox*. DA provided, stained and CT scanned specimens of *Anguilla*. RJB and LBP processed the CT scan data. RJB produced the 3D reconstructions and the anatomical descriptions. RJB made quantitative muscle measurements. RJB wrote the paper. All authors read and provided feedback on the manuscript.

References

Adriaens D, Verraes W (1996a) Ontogeny of cranial musculature in *Clarias gariepinus* (Siluroidei: Clariidae): the adductor mandibulae complex. *J Morphol* **229**, 255–269.

Adriaens D, Verraes W (1996b) Ontogeny of the suspensorial and opercular muscles in *Clarias gariepinus* (Siluroidei: Clariidae), and the consequences for respiratory movements. *Neth J Zool* **47**, 61–89.

Aerts P (1991) Hyoid morphology and movements relative to abducting forces during feeding in *Astatotilapia elegans* (Teleostei: Cichlidae). *J Morphol* **208**, 323–345.

Alfaro ME, Janovetz J, Westneat MW (2001) Motor control across trophic strategies: muscle activity of biting and suction feeding fishes. *Am Zool* **41**, 1266–1279.

Anker GC (1974) Morphology and kinetics of the head of the stickleback, *Gasterosteus aculeatus*. *Trans Zool Soc London* **32**, 311–416.

Barel CDN (1982) Towards a constructional morphology of cichlid fishes (Teleostei, Perciformes). *Neth J Zool* **33**, 357–424.

Bouilliart M, Tomkiewicz J, Lauesen P, et al. (2015) Musculoskeletal anatomy and feeding performance of pre-feeding engyodontic larvae of the European eel (*Anguilla anguilla*). *J Anat* **227**, 325–340.

Camp AL, Brainerd EL (2014) Role of axial muscles in powering mouth expansion during suction feeding in largemouth bass (*Micropterus salmoides*). *J Exp Biol* **217**, 1333–1345.

Camp AL, Brainerd EL (2015) Reevaluating musculoskeletal linkages in suction-feeding fishes with X-ray reconstruction of moving morphology (XROMM). *Integr Comp Biol* **55**, 36–47.

Camp AL, Roberts TJ, Brainerd EL (2015) Swimming muscles power suction feeding in largemouth bass. *Proc Natl Acad Sci* **112**, 8690–8695.

Cox PG, Faulkes CG (2014) Digital dissection of the masticatory muscles of the naked mole-rat, *Heterocephalus glaber* (Mammalia, Rodentia). *PeerJ* **2**, e448.

Cox PG, Jeffery N (2011) Reviewing the morphology of the jaw-closing musculature in squirrels, rats, and guinea pigs with contrast-enhanced microCt. *Anat Rec* **294**, 915–928.

Cox PG, Fagan MJ, Rayfield EJ, et al. (2011) Finite element modelling of squirrel, guinea pig and rat skulls: using geometric morphometrics to assess sensitivity. *J Anat* **219**, 696–709.

Datovo A, Vari RP (2013) The jaw adductor muscle complex in teleostean fishes: evolution, homologies and revised nomenclature (Osteichthyes: Actinopterygii). *PLoS ONE* **8**, e60846.

Datovo A, Vari RP (2014) The adductor mandibulae muscle complex in lower teleostean fishes (Osteichthyes: Actinopterygii): comparative anatomy, synonymy, and phylogenetic implications. *Zool J Linn Soc* **171**, 554–622.

Day SW, Higham TE, Holzman R, et al. (2015) Morphology, kinematics, and dynamics: the mechanics of suction feeding in fishes. *Integr Comp Biol* **55**, 21–35.

De Meyer J, Goethals T, Wassenbergh SV, et al. (2018a) Dimorphism throughout the European eel's life cycle: are ontogenetic changes in head shape related to dietary differences? *J Anat* **233**, 289–301.

De Meyer J, Herrel A, Belpaire C, et al. (2018b) Broader head, stronger bite: *in vivo* bite forces in European eel *Anguilla anguilla*. *J Fish Biol* **92**, 268–273.

De Meyer J, Wassenbergh SV, Bouilliart M, et al. (2018c) Built to bite? Differences in cranial morphology and bite performance between narrow- and broad-headed European glass eels. *J Morphol* **279**, 349–360.

De Schepper N, Adriaens D, De Kegel B (2005) *Moringua edwardsi* (Moringuidae: Anguilliformes): cranial specialization for head-first burrowing? *J Morphol* **266**, 356–368.

De Schepper N, Van Liefferinge C, Herrel A, et al. (2007) Cranial musculature of *Anguilla anguilla* (Anguilliformes): functional implications related to narrow-headedness and broad-headedness. In: *Evolutionary Morphology of Body Elongation in Teleosts: Aspects of Convergent Evolution* (ed. De Schepper N), pp. 129–140. PhD Thesis, Ghent University, Ghent, Belgium.

Descamps E, Sochacka A, De Kegel B, et al. (2014) Soft tissue discrimination with contrast agents using micro-CT scanning. *Belg J Zool* **144**, 20–40.

Dutel H, Herbin M, Clément G, et al. (2015) Bite force in the extant coelacanth Latimeria: the role of the intracranial joint and the basicranial muscle. *Curr Biol* **25**, 1228–1233.

Eschmeyer WN, Fong JD (2013) Species by family/subfamily. Cat. Fishes Electron. Version See http://researcharchive.calacademy.org/research/ichthyology/catalog/SpeciesByFamily.asp Accessed 25 March 2013.

Ferry LA, Paig-Tran EM, Gibb AC (2015) Suction, ram, and biting: deviations and Limitations to the capture of aquatic prey. *Integr Comp Biol* **55**, 97–109.

Geerinckx T, Adriaens D (2007) Ontogeny of the intermandibular and hyoid musculature in the suckermouth armoured catfish Ancistrus cf. triradiatus (Loricariidae, Siluriformes). *Anim Biol* **57**, 339–357.

Gignac PM, Kley NJ, Clarke JA, et al. (2016) Diffusible iodine-based contrast-enhanced computed tomography (diceCT): an emerging tool for rapid, high-resolution, 3-D imaging of metazoan soft tissues. *J Anat* **228**, 889–909.

Goulet CL, Smith HJ, Maie T (2016) Comparative lever analysis and ontogenetic scaling in esocid fishes: functional demands and constraints in feeding biomechanics. *J Morphol* **277**, 1447–1458.

Greenwood PH (1971) Hyoid and Ventral Gill Arch Musculature in Osteoglossomorph Fishes. *Bull br Mus nat Hist Zool.* **22**, 1–55.

Gregory WK (1933) Fish skulls: a study in the evolution of natural mechanisms. *Trans Am Philos Soc* **23**, 76–481.

Helfman GS, Clark JB (1986) Rotational feeding: overcoming gape-limited foraging in anguillid eels. *Copeia* **1986**, 679–685.

Helfman G, Collette BB, Facey DE, et al. (2009) *The Diversity of Fishes: Biology, Evolution, and Ecology*. Hoboken: John Wiley.

Herrel A, Adriaens D, Verraes W, et al. (2002) Bite performance in clariid fishes with hypertrophied jaw adductors as deduced by bite modeling. *J Morphol* **253**, 196–205.

Holliday CM, Tsai HP, Skiljan RJ, et al. (2013) A 3D interactive model and atlas of the jaw musculature of alligator mississippiensis. *PLoS ONE* **8**, e62806.

Huysentruyt F, Geerinckx T, Adriaens D (2007) A descriptive myology of Corydoras aeneus (Gill, 1858)(Siluriformes: Callichthyidae), with a brief discussion on adductor mandibulae homologies. *Anim Biol* **57**, 433–452.

Ide C, Schepper ND, Christiaens J, et al. (2011) Bimodality in head shape in European eel. *J Zool* **285**, 230–238.

Jeffery NS, Stephenson RS, Gallagher JA, et al. (2011) Micro-computed tomography with iodine staining resolves the arrangement of muscle fibres. *J Biomech* **44**, 189–192.

Lauder GV (1980) Evolution of the feeding mechanism in primitive actionopterygian fishes: a functional anatomical analysis of Polypterus, Lepisosteus, and Amia. *J Morphol* **163**, 283–317.

Lauder GV (1982) Patterns of evolution in the feeding mechanism of actinopterygian fishes. *Am Zool* **22**, 275–285.

Lauder GV (1985) Aquatic feeding in lower vertebrates. In: *Functional Vertebrate Morphology* (eds Hildebrand M, Bramble DM, Liem KF, Wake DB), pp. 210–229. Cambridge: Harvard University Press.

Lauder GV, Norton SM (1980) Asymmetrical muscle activity during feeding in the Gar, *Lepisosteus oculatus*. *J Exp Biol* **84**, 17–32.

Lautenschlager S (2013) Cranial myology and bite force performance of Erlikosaurus andrewsi: a novel approach for digital muscle reconstructions. *J Anat* **222**, 260–272.

Lautenschlager S, Bright JA, Rayfield EJ (2014) Digital dissection – using contrast-enhanced computed tomography scanning to elucidate hard- and soft-tissue anatomy in the Common Buzzard *Buteo buteo*. *J Anat* **224**, 412–431.

Leysen H, Christiaens J, De Kegel B, et al. (2011) Musculoskeletal structure of the feeding system and implications of snout elongation in *Hippocampus reidi* and *Dunckerocampus dactyliophorus*. *J Fish Biol* **78**, 1799–1823.

Liem KF (1980a) Acquisition of energy by teleosts: adaptive mechanisms and evolutionary patterns. In: *Environmental Physiology of Fishes* (ed. Ali MA), pp. 299–334. Berlin: Springer.

Liem KF (1980b) Adaptive significance of intra- and interspecific differences in the feeding repertoires of cichlid fishes. *Am Zool* **20**, 295–314.

Liem KF (1990) Aquatic versus terrestrial feeding modes: possible impacts on the trophic ecology of vertebrates. *Am Zool* **30**, 209–221.

Mehta RS, Wainwright PC (2007a) Biting releases constraints on moray eel feeding kinematics. *J Exp Biol* **210**, 495–504.

Mehta RS, Wainwright PC (2007b) Raptorial jaws in the throat help moray eels swallow large prey. *Nature* **449**, 79–82.

Nelson JS (2006) *Fishes of the World*. Hoboken: John Wiley.

Orsbon CP, Gidmark NJ, Ross CF (2018) Dynamic musculoskeletal functional morphology: integrating diceCT and XROMM. *Anat Rec* **301**, 378–406.

Osse JWM (1968) Functional morphology of the head of the perch (*Perca fluviatilis* L.): an electromyographic study. *Neth J Zool* **19**, 289–392.

Porro LB, Richards CT (2017) Digital dissection of the model organism *Xenopus laevis* using contrast-enhanced computed tomography. *J Anat* **231**, 169–191.

Proman JM, Reynolds JD (2000) Differences in head shape of the European eel, *Anguilla anguilla* (L.). *Fish Manag Ecol* **7**, 349–354.

Rand DM, Lauder GV (1981) Prey capture in the chain pickerel, *Esox niger*: correlations between feeding and locomotor behavior. *Can J Zool* **59**, 1072–1078.

Sharp AC, Trusler PW (2015) Morphology of the jaw-closing musculature in the common wombat (*Vombatus ursinus*) using digital dissection and magnetic resonance imaging. *PLoS ONE* **10**, e0117730.

Turingan RG, Wainwright PC (1993) Morphological and functional bases of durophagy in the queen triggerfish, *Balistes vetula* (Pisces, Tetraodontiformes). *J Morphol* **215**, 101–118.

Van Wassenbergh S (2005) A test of mouth-opening and hyoid-depression mechanisms during prey capture in a catfish using high-speed cineradiography. *J Exp Biol* **208**, 4627–4639.

Van Wassenbergh S, Aerts P, Adriaens D, et al. (2005) A dynamic model of mouth closing movements in clariid catfishes: the role of enlarged jaw adductors. *J Theor Biol* **234**, 49–65.

Van Wassenbergh S, Herrel A, Adriaens D, et al. (2007a) No trade-off between biting and suction feeding performance in clariid catfishes. *J Exp Biol* **210**, 27–36.

Van Wassenbergh S, Herrel A, Adriaens D, et al. (2007b) Interspecific variation in sternohyoideus muscle morphology in clariid catfishes: functional implications for suction feeding. *J Morphol* **268**, 232–242.

Vickerton P, Jarvis J, Jeffery N (2013) Concentration-dependent specimen shrinkage in iodine-enhanced microCT. *J Anat* **223**, 185–193.

Wainwright PC, Bellwood DR, Westneat MW, et al. (2004) A functional morphospace for the skull of labrid fishes: patterns of diversity in a complex biomechanical system. *Biol J Linn Soc* **82**, 1–25.

Wainwright PC, McGee MD, Longo SJ, et al. (2015) Origins, innovations, and diversification of suction feeding in vertebrates. *Integr Comp Biol* **55**, 134–145.

Westneat MW (2004) Evolution of levers and linkages in the feeding mechanisms of fishes. *Integr Comp Biol* **44**, 378–389.

Westneat MW (2006) Skull biomechanics and suction feeding in fishes. In: *Fish Biomechanics, Fish Physiology Series* (eds Lauder GV, Shadwick RE), pp. 29–76. New York, NY: Academic Press.

Winterbottom R (1973) A descriptive synonymy of the striated muscles of the teleostei. *Proc Acad Nat Sci Phila* **125**, 225–317.

Supporting Information

Additional Supporting Information may be found in the online version of this article:

Table S1. Summary table of muscle origins and insertions in *Esox* and *Anguilla*.

Table S2. Supplementary data tables of raw and scaled muscles measurements for *Esox* and *Anguilla*.